Energy-Versus-Bandwidth-Efficiency Tradeoff in Spatially Modulated Massive MIMO Downlink

Momo Arisaka, *Student Member, IEEE*, and Shinya Sugiura, *Senior Member, IEEE*

***Abstract*—In this paper, we investigate the effects of pulse shaping on the bandwidth-versus-energy-efficiency tradeoff of band-limited spatial modulation (SM) massive multiple-input multiple-output (MIMO) systems. Although single-RF SM schemes have the merit of achieving high energy and bandwidth efficiencies, owing to the benefits of its antenna-activation principle, most of the previous studies assumed the use of a time-orthogonal shaping filter, which is unrealistic for a single-RF SM transmitter. To this end, we consider the use of time-limited shaping filters, such as a truncated root-raised cosine filter and a truncated Gaussian filter, for the single-RF SM transmitter. Our information-theoretic results demonstrate that, unlike in the previous studies, single-RF SM schemes do not exhibit any substantial advantages over the conventional full-RF MIMO schemes for a low number of transmit antennas, while for a large-scale antenna array, single-RF SM schemes outperform the conventional full-RF MIMO schemes.**

***Index Terms*—Antenna activation, bandwidth and energy efficiency, Gaussian filter, pulse shaping, spatial modulation.**

I. Introduction

Spatial modulation (SM) [1–4] has been recognized as the fifth multiple-antenna multiple-output (MIMO) technique, in addition to the four conventional spatial multiplexing (SMX), space-time coding, beamforming, and space-division multiple access. The principle of SM is that only one of multiple antenna elements is activated in each symbol interval, where the activated antenna index conveys information bits beyond those in the classic modulation scheme. Hence only a single RF branch is needed at the SM transmitter, despite the use of multiple antenna elements. Although the peak data rate of SM is lower than that of SMX when assuming the same number of transmit antenna elements, a SM scheme's transmission rate logarithmically increases upon linearly increasing the number of transmit antenna elements.

One of the most important benefits of SM over SMX is that a high-level tradeoff between energy and bandwidth efficiencies is achievable. As mentioned in [1, 2, 5], in the conventional full-RF SMX transmitter, the static power consumption imposed by the circuit, including the power amplifier, linearly increases with the number of transmit antenna elements. More specifically, in [5], it was clarified for the first time that full-RF MIMO systems may be less energy efficient than their single-antenna counterparts when both the dynamic and static power consumptions are considered in a fair manner. Note that in [5], the performance comparisons were provided in terms of mutual information, whereas the SM scheme's antenna activation process was not taken into account in the analysis, for the sake of simplicity.

One fundamental limitation imposed on SM is that the SM transmitter has to employ a bandwidth-inefficient time-limited shaping filter, because of the antenna switching mechanism of the SM concept [2, 6, 7]. The need for the time-limited pulse shaping was mentioned in [6], while in [7], a fair comparison between SM and SMX was first carried out in terms of bandwidth efficiency. However, the effects of time-limited pulse shaping on the energy efficiency have not been presented before, despite a high energy efficiency being one of the most important claims of SM. Note that in most SM studies other than [6, 7], these detrimental effects have been typically ignored.

Against this background, the novel contributions of this paper are as follows. We first introduce a framework that allows us to demonstrate the tradeoff between the energy and bandwidth efficiencies of SM, which is compared with the existing full-RF MIMO benchmarks in a fair manner by taking into account the effects of time-limited pulse shaping, which is specific to SM. The performance results are provided in terms of mutual information by considering specific time-limited shaping filters, namely, a truncated root-raised cosine (RRC) filter and a truncated Gaussian filter, in addition to an ideal (unrealistic) sinc pulse filter. We demonstrate the above-mentioned benefits of SM in a massive MIMO scenario for the first time, where the number of transmit antenna elements at the SM base station is significantly high.[1]

II. System Model

We consider an SM-aided downlink scenario where a base station equipped with $N_{\rm tx}$ transmit antennas sends information bits to a single user, and we assume a frequency-flat Rayleigh fading channel. The base station activates a single transmit antenna per symbol interval, and a modulated symbol is transmitted from the activated transmit antenna element. Hence, both an index of transmit antenna elements and a modulated symbol are used for conveying $\log_2 N_{\rm tx}$ and $\log_2 \mathcal{M}$ information bits, respectively, where $\mathcal{M}$ indicates the modulation size [2].

Assuming that the user has $N_{\rm rx}$ receive antenna elements, the received signals $\mathbf{y} \in \mathbb{C}^{N_{\rm rx}}$ are represented by $\mathbf{y} = \mathbf{H}\mathbf{s} + \mathbf{n}$,

M. Arisaka is with the Department of Computer and Information Sciences, Tokyo University of Agriculture and Technology, Koganei, Tokyo 184-8588, Japan. S. Sugiura is with the Institute of Industrial Science, University of Tokyo, Meguro-ku, Tokyo 153-8505, Japan (e-mail: sugiura@ieee.org). (*Corresponding Author: Shinya Sugiura.*) This work was supported in part by the Japan Society for the Promotion of Science (JSPS) KAKENHI Grant Numbers 26709028, 16KK0120, and 17K18871.

[1]The framework of [5] does not support the antenna activation of SM, and hence it was impossible to evaluate SM in the context of massive MIMO.

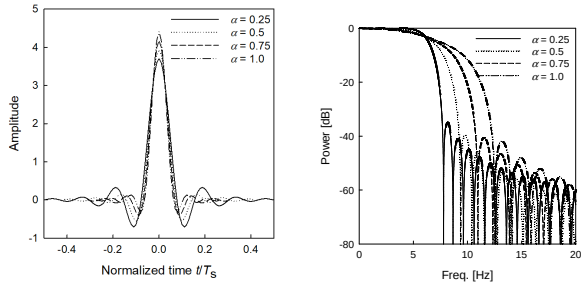

(a) Time domain (b) Frequency domain

Fig. 1. Time- and frequency-domain impulse responses of the truncated RRC filter, where $T_{\rm s} = 1.0$ s.

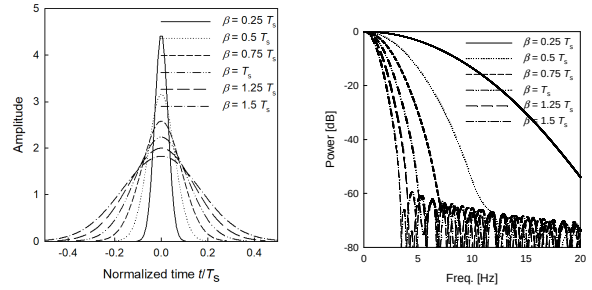

(a) Time domain (b) Frequency domain

Fig. 2. Time- and frequency-domain impulse responses of the truncated Gaussian filter, where $T_{\rm s} = 1.0$ s.

where $\mathbf{H} = [\mathbf{h}_1, \cdots, \mathbf{h}_{N_{\rm tx}}] \in \mathbb{C}^{N_{\rm rx} \times N_{\rm tx}}$ represents the MIMO channel coefficients, and $\mathbf{n}$ denotes the additive white Gaussian noise (AWGN) components. Furthermore, $\mathbf{s} \in \mathbb{C}^{N_{\rm tx}}$ is the SM symbol vector, which only contains a single non-zero component, namely, the one associated with the activated transmit antenna element. The index of the active transmit antenna is m $(m = 1, \cdots, N_{\rm tx})$.

A. Time-Limited Shaping Filter

Owing to the concept of single antenna activation, the base station only has to be equipped with a single RF branch. However, in order to benefit from this, the symbol duration has to be shorter than the symbol interval [2], and hence a time-limited shaping filter, rather than a time-orthogonal one, has to be employed [7].

In this paper, we consider two types of time-limited shaping filters applicable to a single-RF SM transmitter, namely, a truncated RRC filter and a truncated Gaussian filter, where the time-domain impulse responses are truncated outside a symbol interval, such that the total power of each pulse is concentrated within the range $[-T_{\rm s}/2,\ T_{\rm s}/2]$. The time- and frequency-domain impulse responses of the truncated RRC and Gaussian filters are shown in Figs. 1 and 2, respectively. The parameters are respectively α, the roll-off factor, and β, which corresponds to a spectral efficiency, given by $\beta = \sqrt{2 \ln 2}/(BT_{\rm s})$, where B is the 3-dB bandwidth [8]. The 3-dB, 10-dB, and 20-dB cut-off bandwidths calculated from Figs. 1 and 2 are listed in Table I; these bandwidths are used in the performance comparisons of Section III. Note that the cut-off bandwidth of the truncated Gaussian filter with a sufficiently high β is typically lower than that of the truncated RRC filter.

TABLE I
CUT-OFF BANDWIDTH OF TRUNCATED RRC AND GAUSSIAN FILTERS

(a) RRC filter

parameter α	0.25	0.5	0.75	1.0
3 dB	12.02	11.91	11.91	12.05
10 dB	13.68	15.51	17.31	19.15
20 dB	14.69	17.20	19.78	22.36

(b) Gaussian filter

parameter β	0.25	0.5	0.75	1.0	1.25	1.5
3 dB	9.41	4.71	3.14	2.36	1.89	1.57
10 dB	17.17	8.58	5.72	4.29	3.43	2.86
20 dB	24.28	12.14	8.09	6.07	4.85	4.04

B. Bandwidth Efficiency

The average information rate of a single-RF SM scheme is formulated as [5, 9]

$$\mathcal{C} = W(\mathcal{C}_1 + \mathcal{C}_2), \tag{1}$$

where W is the bandwidth of a truncated shaping filter, which is calculated by dividing the available bandwidth by the cut-off bandwidth shown in Table I. Then, we have mutual information as follows:

$$\mathcal{C}_1 = \mathrm{I}(\mathbf{s}; \mathbf{y}|m) \tag{2}$$

$$= \frac{1}{N_{\rm tx}} \sum_{i=1}^{N_{\rm tx}} \log_2 \left(1 + \frac{P\|\mathbf{h}_i\|^2}{N_0}\right), \tag{3}$$

$$\mathcal{C}_2 = \mathrm{I}(\mathbf{y}; m), \tag{4}$$

in which P is the average symbol power, and $\mathcal{C}_1$ denotes the capacity related to a modulated non-zero symbol in $\mathbf{s}$, which is assumed to be complex-valued Gaussian distributed. Furthermore, $\mathcal{C}_2$ corresponds to the mutual information provided by antenna activation. As mentioned in [5], it is a challenging task to calculate the mutual information (4), in terms of calculation cost, especially when the number of transmit antenna elements $N_{\rm tx}$ is high.

Instead, let us consider a lower bound of $\mathcal{C}_2$, $\mathrm{I}(\hat{m}; m)$ [10], which is formulated as

$$\mathrm{I}(\hat{m}; m) = \frac{1}{N_{\rm tx}} \sum_{m=1}^{N_{\rm tx}} \sum_{k=1}^{N_{\rm tx}} \mathrm{P}(k|m) \log_2 \frac{N_{\rm tx}\mathrm{P}(k|m)}{\sum_{l=1}^{N_{\rm tx}} \mathrm{P}(k|l)}, \tag{5}$$

where

$$\mathrm{P}(k|m) = \exp\left(-\frac{\gamma_{k-1,k}}{2\sigma_m^2}\right) - \exp\left(-\frac{\gamma_{k,k+1}}{2\sigma_m^2}\right), \tag{6}$$

and $\hat{m}$ is an index of antenna activation, which is detected based on $\mathbf{y}$. Also, we have $\gamma_{0,1} = 0, \gamma_{N_{\rm tx},N_{\rm tx}+1} = \infty$, and

$$\gamma_{k,l} = \frac{\sigma_k^2 \sigma_l^2}{\sigma_l^2 - \sigma_k^2} \ln \frac{\sigma_l^2}{\sigma_k^2}, \quad (1 \le k, l \le N_{\rm tx}) \tag{7}$$

$$\sigma_m^2 = P\|\mathbf{h}_m\|^2 + N_0. \quad (1 \le m \le N_{\rm tx}). \tag{8}$$

Moreover, the upper bound of $\mathcal{C}_2$ is simply given by

$$\mathcal{C}_2 \le \log_2 N_{\rm tx}, \tag{9}$$

which represents the maximum achievable rate associated with

antenna activation of SM. Finally, from (1), (5), and (9), the information rate of SM is upper and lower bounded as follows:

$$\mathcal{C}_{\min} \leq \mathcal{C} \leq \mathcal{C}_{\max}, \tag{10}$$

where we have $\mathcal{C}_{\min} = W\left[\mathcal{C}_1 + \mathrm{I}(\hat{\mathrm{X}}_{\mathrm{ch}}; \mathrm{X}_{\mathrm{ch}})\right]$ and $\mathcal{C}_{\max} = W(\mathcal{C}_1 + \log_2 N_{\mathrm{tx}})$.

C. Energy Efficiency

According to the EARTH power model [5], the total power consumption at a general MIMO-aided base station is expressed as an affine function of the RF transmit power as follows:

$$P_{\mathrm{supply}} = \begin{cases} N_{\mathrm{RF}} P_0 + \zeta N_{\mathrm{RF}} P_{\mathrm{t}}, & 0 < P_{\mathrm{t}} \leq P_{\max} \\ P_{\mathrm{sleep}}, & P_{\mathrm{t}} = 0 \end{cases}, \tag{11}$$

where P_{supply} denotes the total power supplied to the base station, while N_{RF} denotes the number of RF chains at the base station and P_0 is the minimum power consumption per RF chain. Furthermore, ζ is the slope of the load-dependent power consumption, P_{t} is the RF transmit power per antenna element, $P_{\max}$ is the maximum transmitted power per antenna, and P_{sleep} represents the power consumption in sleep mode. Note that we have $N_{\mathrm{RF}} = 1$ for a single-RF SM base station, and hence its total power consumption (11) may be significantly lower than that of a full-RF MIMO-aided base station, especially when the number of antenna elements is high.

The total power of the single-RF SM transmitter $P^{\mathrm{SM}}_{\mathrm{supply}}$ and that of the full-RF MIMO transmitter $P^{\text{Full-RF}}_{\mathrm{supply}}$ have the relationship $P^{\mathrm{SM}}_{\mathrm{supply}} = P^{\text{Full-RF}}_{\mathrm{supply}} - (N_{\mathrm{RF}} - 1)P_0$, where $P^{\mathrm{SM}}_{\mathrm{supply}}$ denotes the total power supply of single-RF SM and $P^{\text{Full-RF}}_{\mathrm{supply}}$ is that of full-RF MIMO. Additionally, the energy efficiency of a base station is defined by $\mathrm{EE} = \mathcal{C}/P_{\mathrm{supply}}$ [5].

III. Performance Results

In this section, we provide our performance results, in order to characterize the energy and bandwidth efficiencies of the single-RF SM base station, from Monte Carlo simulations. In our simulations, the number of transmit antennas at the base station, N_{tx}, was varied between 4 and 128, and a single antenna element at the mobile receiver was considered. Furthermore, the distance between the base station and the mobile receiver was generated randomly between $d_{\min}$ and $d_{\max}$ according to a uniform distribution. We employed the 3GPP NLOS [11] model for the path loss, while the shadowing standard deviation was set to 6 dB, which corresponds to the scenario of an urban macro base station. The noise variance was given by $N_0 = W\kappa\theta$, where κ is the Boltzmann constant and θ is the operating temperature [5]. The benchmarks are orthogonal space-time block coding (OSTBC) and SMX schemes, each employing a bandwidth-efficient sinc shaping filter, which is available owing to the full-RF transmitter structure. Other parameters used in the simulations are listed in Table II.

Firstly, we investigate the performance for a scenario with $N_{\mathrm{tx}} = 4$ transmit antennas. Figs. 3(a) and 3(b) show the

TABLE II
Simulation Parameters [5]

Simulation Parameter	Values
BS type	Macrocell
Power model	SOTA2010 [12]
Carrier frequency	2 GHz
Path loss	3GPP NLOS [11]
Number of Monte Carlo simulations	100,000
Bandwidth	10 MHz
Operating temperature	290 K (outdoor)

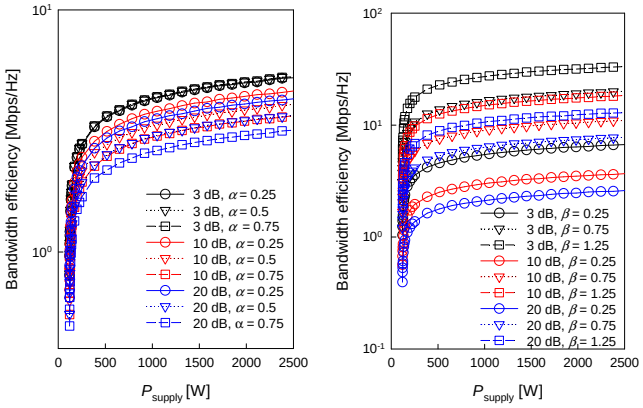

(a) RRC filter (b) Gaussian filter

Fig. 3. Lower bound of bandwidth efficiency for the SM-aided downlink with cut-off bandwidths of 3 dB, 10 dB, and 20 dB; (a) truncated RRC filter with roll-off factor $\alpha = 0.25$, 0.5, and 0.75, and (b) truncated Gaussian filter with parameter $\beta = 0.25$, 0.75, and 1.25.

bandwidth efficiency of the SM-aided downlink, employing the truncated RRC and the truncated Gaussian filters, respectively, while considering cut-off bandwidths of 3 dB, 10 dB, and 20 dB. The roll-off factor of the truncated RRC filter was set to $\alpha = 0.25$, 0.5, and 0.75, while the parameter of the truncated Gaussian filter was set to $\beta = 0.25$, 0.75, and 1.25. Observe in Fig. 3(a) that for the 3-dB bandwidth, the bandwidth efficiency remained almost unchanged, regardless of the α value, while for the 10-dB and 20-dB bandwidths, the bandwidth efficiency increased with decreasing α. It is shown in Fig. 3(b) that, for the truncated Gaussian filter, the bandwidth efficiency increased with increasing α and also had the tendency to exhibit a higher bandwidth efficiency than did the RRC filter as shown in Fig. 3(a).

Next, Fig. 4(a) shows the upper and lower bounds of the bandwidth efficiency for single-RF SM schemes employing the truncated RRC filter with $\alpha = 0.25$ or the truncated Gaussian filter with $\beta = 1.25$. The benchmark schemes were the full-RF STBC and MISO benchmark schemes employing a sinc filter, where we considered a 3-dB bandwidth; we also plotted the ideal (unpractical) SM scheme employing a sinc filter, for reference. Observe in Fig. 4(a) that the two realistic SM schemes employing truncated filters exhibited unignorable performance penalties in comparison to their ideal SM counterparts. Moreover, the SM scheme employing a truncated Gaussian filter had an advantage over the full-RF

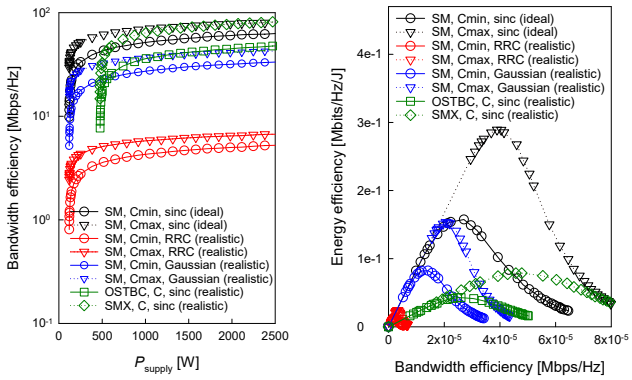

(a) Bandwidth efficiency (b) Energy efficiency

Fig. 4. Upper and lower bounds of the bandwidth and energy efficiencies for single-RF SM schemes with $N_{\text{tx}} = 4$ transmit antennas employing a truncated RRC filter with $\alpha = 0.25$ or a truncated Gaussian filter with $\beta = 1.25$.

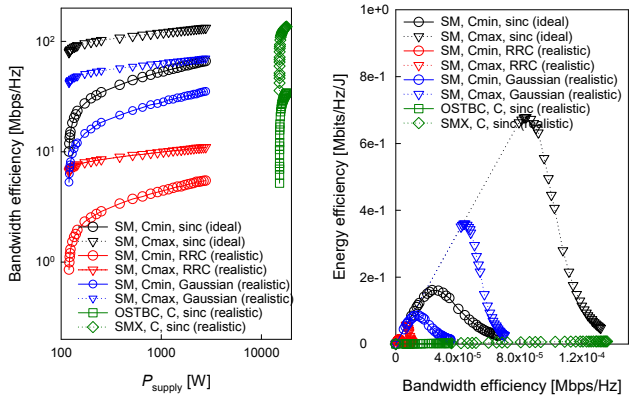

(a) Bandwidth efficiency (b) Energy efficiency

Fig. 5. Upper and lower bounds of the bandwidth and energy efficiencies for single-RF SM schemes with $N_{\text{tx}} = 128$ transmit antennas, employing a truncated RRC filter with $\alpha = 0.25$ or a truncated Gaussian filter with $\beta = 1.25$.

benchmark schemes only in the low-power and low-rate range of approximately $P_{\text{supply}} \leq 500$ W.

Furthermore, Fig. 4(b) shows the tradeoff between the energy and the bandwidth efficiencies with the same system parameter settings as used for Fig. 4(a). The peak energy efficiency of the realistic SM scheme employing the truncated Gaussian filter was higher than those of the full-RF benchmark schemes. However, upon increasing the bandwidth efficiency over 30 Mbps/Hz, this advantage diminished in this low-number-transmit-antenna scenario.

Having investigated the performance of a low-number-transmit-antenna scenario, we next consider the SM scheme employing a large-scale antenna array comprising $N_{\text{tx}} = 128$ antennas. Figs. 5(a) and 5(b) show the achievable performance with the same system parameters as those used in Figs. 4(a) and 4(b), respectively, except for the number of transmit antennas.

It is shown in Fig. 5(b) that the bandwidth efficiency of the realistic SM schemes significantly improved in comparison to that of the $N_{\text{tx}} = 4$ scenario in Fig. 4(a), without requiring a substantial increase of the power supply. By contrast, the full-RF benchmark schemes suffered from needing an excessively high power supply, which is due to the effects of the static power consumed by massive RF chains.

The performance advantages of the SM schemes are more obvious when considering energy efficiency. More specifically, as shown in Fig. 5(b), in terms of energy efficiency, the realistic SM schemes outperformed the full-RF benchmark schemes over the entire calculated bandwidth range.

IV. Conclusions

In this paper, the effects of pulse shaping on the energy and bandwidth efficiencies of SM schemes employing realistic truncated RRC and Gaussian filters were investigated. We considered the upper and lower bounds of information rate, which allows us to compare the achievable performance with those of other, full-RF MIMO schemes. Our simulation results demonstrated that, while the performance advantage of SM schemes is limited for a low number of transmit antennas, it significantly increases when considering a massive MIMO downlink. This was achieved as the explicit benefit of an energy-efficient single-RF transmitter structure.

References

[1] M. Di Renzo, H. Haas, A. Ghrayeb, S. Sugiura, and L. Hanzo, "Spatial modulation for generalized MIMO: Challenges, opportunities and implementation," *Proceedings of the IEEE*, vol. 102, no. 1, pp. 1–47, Jan. 2014.

[2] S. Sugiura, T. Ishihara, and M. Nakao, "State-of-the-art design of index modulation in the space, time, and frequency domains: Benefits and fundamental limitations," *IEEE Access*, vol. 5, pp. 21 774–21 790, Nov. 2017.

[3] P. Ju, M. Zhang, X. Cheng, and L. Yang, "Generalized spatial modulation with transmit antenna grouping for massive MIMO," in *IEEE International Conference on Communications*, May 2017, pp. 1–6.

[4] X. Cheng, M. Zhang, M. Wen, and L. Yang, "Index modulation for 5G: Striving to do more with less," *IEEE Wireless Communications*, vol. 25, no. 2, pp. 126–132, Apr. 2018.

[5] A. Stavridis, S. Sinanovic, M. D. Renzo, and H. Haas, "Energy evaluation of spatial modulation at a multi-antenna base station," in *IEEE 78th Vehicular Technology Conference*, Las Vegas, NV, USA, 2–5 Sept. 2013, pp. 1–5.

[6] M. D. Renzo, D. D. Leonardis, F. Graziosi, and H. Haas, "Space shift keying (SSK) MIMO with practical channel estimates," *IEEE Transactions on Communications*, vol. 60, no. 4, pp. 998–1012, Apr. 2012.

[7] K. Ishibashi and S. Sugiura, "Effects of antenna switching on band-limited spatial modulation," *IEEE Wireless Communications Letters*, vol. 3, no. 4, pp. 345–348, Aug 2014.

[8] A. Goldsmith, *Wireless communications*. Cambridge University Press, 2005.

[9] Y. Yang and B. Jiao, "Information-guided channel-hopping for high data rate wireless communication," *IEEE Communications Letters*, vol. 12, no. 4, pp. 225–227, Apr. 2008.

[10] Z. An, J. Wang, J. Wang, S. Huang, and J. Song, "Mutual information analysis on spatial modulation multiple antenna system," *IEEE Transactions on Communications*, vol. 63, no. 3, pp. 826–843, March 2015.

[11] 3rd Generation Partnership Project, "Further advancements for e-utra physical layer aspects (release 9)," Tech. Rep., Sep 2009. [Online]. Available: www.3gpp.org/ftp/Specs/

[12] G. Auer, V. Giannini, I. Godor, P. Skillermark, M. Olsson, M. A. Imran, D. Sabella, M. J. Gonzalez, C. Desset, and O. Blume, "Cellular energy efficiency evaluation framework," in *Proc. of the IEEE Vehicular Technology Conference (VTC Spring)*, May 2011, pp. 1–6.